Selective delipidation of *Mycobacterium bovis BCG* enables direct pulmonary vaccination and enhances protection against *Mycobacterium tuberculosis*

Juan I. Moliva[1,2], **Austin P. Hossfeld**[2], **Sabeen Sidiki**[2], **Cynthia H. Canan**[2], **Varun Dwivedi**[1], **Gillian Beamer**[3], **Joanne Turner**[1,2,*], and **Jordi B. Torrelles**[1,2,*]

[1]Texas Biomedical Research Institute, San Antonio, Texas, 78245, USA

[2]Department of Microbial Infection and Immunity, Wexner College of Medicine, The Ohio State University, Columbus, Ohio, 43210, USA

[3]Department of Infectious Diseases and Global Health, Cummings School of Veterinary Medicine, Tufts University, North Grafton, Massachusetts, 01536, USA

Abstract

Mycobacterium tuberculosis (*M.tb*), the causative agent of tuberculosis (TB), is the leading killer due to an infectious organism. *Mycobacterium bovis* bacillus Calmette-Guérin (BCG) is the only vaccine approved against TB, however, its efficacy against pulmonary TB is poor. While BCG is currently inoculated intradermally, the natural route of *M.tb* infection is through the lung. Excessive lung pathology caused by pulmonary inoculation of BCG has prevented the use of this immunization route. Here, we show that selective chemical treatment of BCG with petroleum ether removes inflammatory lipids from the bacterial surface while keeping BCG viable. Pulmonary vaccination using this modified BCG attenuated inflammatory responses, prevented immunopathology of the lung, and significantly increased protection against *M.tb* infection in mice. We further directly linked IL-17A as the responsible contributor of improved immunity against *M.tb* infection. These results provide evidence that selective removal of cytotoxic lipids from the BCG surface attenuates inflammation and offers a safer and superior vaccine against TB causing less damage post-infectious challenge with *M.tb*.

*Corresponding authors: Dr. Joanne Turner, Texas Biomedical Research Institute, 7620 NW Loop 410, San Antonio, Texas 78227; JoanneTurner@txbiomed.org; and Dr. Jordi B. Torrelles, Texas Biomedical Research Institute, 7620 NW Loop 410, San Antonio, Texas 78227; JTorrelles@txbiomed.org.

INTRODUCTION

Mycobacterium tuberculosis (*M.tb*) the causative agent of tuberculosis (TB) continues to cause significant morbidity and mortality around the world, and the rise of extensive-, extreme-, and total-drug resistant *M.tb* has endangered eradication efforts [1]. The currently licensed vaccine against TB, *Mycobacterium bovis* Bacille Calmette et Guérin (BCG), is only partially effective against pulmonary TB (PTB) despite it being highly efficacious against other forms of mycobacterial disease such as TB meningitis and miliary TB [2,3]. One potential explanation for this discrepancy may lie in the route of immunization as BCG is administered intradermally, whereas *M.tb* is a natural airborne pathogen [4]. This noted disparity may explain why BCG fails to confer optimum anti-mycobacterial immunity in the lung. To circumvent this issue research has shifted toward direct pulmonary vaccination with BCG [5–7]. Evidence suggests that BCG is too pathogenic to be utilized as a direct pulmonary vaccine as it can induce significant pulmonary immunopathology [4,8,9]. For this reason, no human clinical trial has yet been implemented to evaluate the efficacy of pulmonary BCG vaccination against *M.tb*.

The primary reason behind the immunopathology caused by mycobacteria to the lung is attributed to potent inflammatory and immunomodulatory lipids such as trehalose dimycolate (TDM) [10,11], di- and tri-acylglycerols (DAG/sTAGs) [12], phthiocerol dimycocerosates (PDIMs) [13], phenolic glycolipids (PGLs) [14,15], among others, present on the BCG cell wall. These lipids induce rapid and robust innate immune responses that lead to tissue inflammation and damage [16] or are used by mycobacteria to subvert host immunity [13,17–20]. However, recombinant BCG strains deficient in specific lipids or a combination of these lipids are weak inducers of immune responses that protect mice against *M.tb* [21]. Thus, it is suggested that complete absence of the cell wall lipids is detrimental to the generation of immunity, but their presence is responsible for lung pathology. In this study, we recapitulated and extended previous studies by Silva *et al.* [11]. We demonstrated that treatment of BCG with the organic solvent petroleum ether (PE) selectively extracts many of the inflammatory lipids, including TDM, PGL, mycoside B (MycB), and some triacylglycerols (TAGs) and PDIMs without affecting the viability of BCG. Using primary human macrophages, we demonstrate qualitative and quantitative lowered innate inflammatory responses to delipidated BCG (dBCG) compared to conventional BCG. This observation led us to hypothesize that delipidation of BCG could be used as an effective pulmonary vaccine as it would bypass the pathology associated with this route of vaccination while retaining the efficacy associated with direct inoculation of the lung. We show that direct inoculation of the lung with dBCG significantly reduced the inflammatory status of the lung in vaccinated mice compared to conventional BCG. Furthermore, vaccination with dBCG conferred superior protection relative to conventional BCG against challenge with *M.tb*. Protection against *M.tb* infection by dBCG vaccination was associated with increased numbers of effector and central memory T cell populations in the lung, and with increased CD69+ and IL-17A+, but not IFNγ+, T cell responses. Depletion of IL-17A throughout the vaccination period abrogated protection in the lung of dBCG-vaccinated mice. Altogether, our results provide proof of concept that dBCG can be easily adapted into a pulmonary vaccine with few safety concerns and enhanced efficacy against *M.tb*.

RESULTS

Petroleum ether treatment extracts non-polar lipids from BCG without affecting bacillus viability, attenuating innate inflammatory responses

Lipid extraction from PE treated BCG was assessed by thin layer chromatography (TLC). Three independent PE extractions are shown (PE BCG Extract). BCG total lipids were included on TLCs as controls. To assess the amount and the makeup of the remaining lipids on BCG after PE extraction, bacteria were further extracted with chloroform:methanol (2:1, v/v) (C:M BCG Extract). As described [11,22–24], TDM was highly extractable using PE resulting in a consistent removal of 70%–90% TDM from BCG (Fig. 1A, D). Due to the hydrophobic nature of PE, we also observed significant extraction of PGL and MycB, both important virulence factors associated with the mycobacterial cell wall (Fig.1A, D). Additionally, some PDIMs and TAGs were partially extractable (Fig.1B, D). As expected, PE was unable to remove phospholipids such as phosphatidyl-*myo*-inositol mannosides (PIMs) from the BCG cell wall, and PIMs were only extractable after C:M extraction (Fig. 1E, D). We further confirmed that large chain carbohydrates such as mannose-capped lipoarabinomannan (ManLAM) were not directly or indirectly extractable with PE (see Sup. Fig.S1A) and remained on the PE treated BCG cell wall (see Sup. Fig.S1B).

To confirm that lipid extraction by PE was not lethal or inhibitory for optimal growth of BCG, we plated PBS-treated, PE-treated, or PE+C:M-treated BCG. As previously described [11,22], no significant differences in growth between PBS and PE treated BCG was observed, whereas PE+C:M-treated BCG did not grow (Fig.1E). We confirmed that delipidation of BCG (dBCG) generated a single cell suspension of bacteria (see Sup. Fig.S2). Therefore, PE extracted a significant portion of cytotoxic, non-polar molecules from the BCG cell wall with high reproducibility, and without affecting BCG viability.

The consequence of removing non-polar lipids on the viability and innate inflammatory responses of BCG was first determined *in vitro* in primary human macrophages. Despite equal inoculums (Fig. S3A), BCG and dBCG had an average uptake of 9.66 ± 5.51 and 3.00 ± 1.32 (M ± SD), respectively, suggesting that non-polar lipids may directly impact the interaction between BCG and human macrophages. Growth of dBCG in macrophages was significantly reduced when compared to conventional BCG (Fig.S3B), and dBCG inoculated macrophages released significantly less TNF, IL-1β, IL-6, and IL-10, but not IL-12p40 (Fig.S3C, D), supporting previous findings using delipidated *M.tb*, where both cytokine reduction in spite of better bacterial killing was also observed [22]. Moreover, lower levels of secreted lactose dehydrogenase (LDH) were detected in dBCG inoculated macrophages (Fig.S3E). Images of dBCG inoculated macrophages captured at 120h post infection corroborated these findings (Fig.S3F).

Delipidation of BCG attenuates pulmonary inflammation in vivo following intranasal vaccination and alters cell populations of the lung

Our *in vitro* data indicate that removal of non-polar lipids reduced inflammatory cytokine secretion (Fig.S3) and therefore we next sought to evaluate the potential of dBCG as a pulmonary vaccine. C57BL/6 mice were inoculated intranasally with 5.0×10^5 BCG or

dBCG bacilli. Despite equal inoculums (Fig.2A), the ability of dBCG to persist in the lung was significantly reduced by day 2 post vaccination (DPV), a trend that continued for up to 150 days, with a continuous decrease in bacteria burden (Fig.2B). By 150 DPV, CFUs in the lung of dBCG-vaccinated mice were below accurate detection levels, whereas BCG-vaccinated mice had higher CFUs in the lung (Fig.2B). The levels of TNF and IL-6 in the lungs of dBCG-vaccinated mice were significantly decreased as early as 7 DPV and the levels of IL-1β, IL-10, and IFNγ displayed the same trend (Sup. Fig.S4). By 50 DPV, all measured cytokines except for IL-12p40 were significantly decreased in the dBCG group. Altogether, the data suggest that chemical removal of non-polar lipids from the BCG cell wall significantly impacts its ability to persist *in vivo* and diminishes inflammatory responses within the lung. To corroborate this, we analyzed the immunopathology of the lung in BCG- or dBCG-vaccinated mice. Lung inflammation was determined by quantifying the size of the inflammatory foci over the total area of the lung lobe. The lung of BCG-vaccinated mice had more extensive areas of inflammation and cellular infiltration compared to dBCG-vaccinated mice at 7 DPV (Fig.2C, D). This same trend was observed at 21 and 50 DPV with larger foci visible in BCG-vaccinated mice compared to dBCG-vaccinated animals. By 150 DPV, inflammation in the lung of BCG-vaccinated mice had decreased but remained significantly higher compared to dBCG-vaccinated mice. Together, the data suggest that dBCG induces immunopathology to a lesser degree than BCG when it is administered directly into the lung, and thus could be a safe pulmonary vaccine.

We assessed immune cell kinetics in the lung of vaccinated mice across 50 days (for gating scheme see Sup. Fig.S5A). Early post vaccination we found significantly reduced percentages of monocytes and neutrophils in the lung of mice vaccinated with dBCG relative to BCG (Sup. Fig.S6A, B). We observed no significant difference in the percentages of alveolar macrophages (AMs) and dendritic cells (DCs) in the lung between groups (Sup. Fig.S6C, D), however, the percentage of AMs decreased significantly from 7 to 21 and 50 DPV. The percentage of DCs increased over time in both groups relative to naïve mice and were found to be significantly elevated in the lung of dBCG vaccinated mice at 50 DPV. We found that B cell numbers increased significantly across time in both vaccination groups (Sup. Fig.S6E). The number of NK cells decreased across time but was significantly increased in BCG-vaccinated mice relative to dBCG-vaccinated mice at 50 DPV (Sup. Fig.S6F), while the percentage of γδ+ T cells was not affected by either formulation, despite overall significant increases across time (Sup. Fig.S6G).

Pulmonary vaccination with dBCG increases memory T cell populations in the lung

BCG is the only licensed vaccine that is thought to primarily mediate protection via the action of memory CD4+ and to a lesser extent CD8+ T cells [25] that respond rapidly upon infection with *M.tb* [26]. For these reasons, we next focused on the proportions of CD4+ and CD8+ T cells expressing markers associated with effector memory (T_{EM} – CD62L-CD44+) and central memory (T_{CM} – CD62L+CD44+) in the lung of BCG- and dBCG-vaccinated mice. The proportion of CD4+ and CD8+ T cells increased across time following vaccination with BCG and dBCG vaccinated mice, but mice vaccinated with dBCG had significantly increased numbers of CD4+ and CD8+ T cells in the lung at 50 DPV (Fig.3A, B and Sup. Fig.S5B). Proportions of T_{EM} CD4+ and CD8+ cells in the lung increased across time in

BCG and dBCG vaccinated mice, with dBCG having significantly more CD4$^+$ T$_{EM}$ at 50 DPV (Fig.3C, D). T$_{EM}$ cells are believed to possess short-lived immunological memory, while tissue-resident T$_{CM}$ cells, though far fewer than T$_{EM}$ in tissue, are longer-lived [27]. We found that dBCG induced greater proportions of CD4$^+$ and CD8$^+$ T$_{CM}$ cells in the lung compared to BCG vaccination (Fig.3E, F).

M.tb challenge after pulmonary vaccination with dBCG attenuates pulmonary immunopathology and affords superior protection relative to conventional BCG

To replace the current TB vaccine, the new candidate must be more efficacious at reducing *M.tb* bacterial burden and preventing TB pathology. Mice were randomized into vehicle (saline), BCG, or dBCG groups and vaccinated with 5×10^5 bacteria via intranasal inoculation of the lung. Fifty days post vaccination, all groups were infected simultaneously with a low dose aerosol of *M.tb* [28]. Bacterial burden was assessed in the lung, spleen, liver, and mediastinal lymph node (MLN) at 21, 60, and 150-days post-infection (DPI). We observed a significant decrease in lung bacterial burden at every time point in mice vaccinated with dBCG, compared to vehicle control and conventional BCG (Fig.4A). We also observed a significant delay in colonization of the spleen (Fig.4B), liver (Fig.4C), and MLN (Fig.4D) in dBCG-vaccinated mice. Together, these data suggest that removal of non-polar lipids from BCG augments its efficacy as a vaccine against *M.tb* by delaying its expansion.

Importantly, we determined if dBCG vaccination was able to reduce tissue damage by quantifying areas of cellular aggregation relative to the total size of the lung (Fig.5). dBCG vaccination attenuated pulmonary inflammation at every time point studied. At 21 DPI small areas of cellular aggregation were visible in all three groups, but foci in the lung of vehicle-vaccinated and BCG mice were significantly larger compared to dBCG (Fig.5A, B). Inflammatory foci doubled in size in the lung of vehicle-treated and BCG vaccinated mice at 60 DPI, whereas foci in the lung of dBCG-vaccinated mice remained small. We also observed significantly decreased pulmonary inflammation in the lung of dBCG-vaccinated mice compared to BCG-vaccinated mice at this time point. At 150 DPI, the mean area of the inflammatory foci was $20.84 \pm 4.66\%$ in vehicle-treated mice and $19.14 \pm 13.54\%$ in BCG-vaccinated mice, whereas in dBCG-vaccinated was $8.30 \pm 3.04\%$. Importantly, the decrease in lung pathology was not due to a reduction in *M.tb* bacterial burden (Sup. Fig.S7A, B). Together the data suggest that dBCG is effective at reducing initial bacterial burden and at delaying pulmonary immunopathology.

Pulmonary vaccination with dBCG accelerates effector T cell responses in the lung upon challenge with M.tb

Next, we evaluated effector T cells responses in the lung of mice that had been vaccinated (DPV 50) or vaccinated and then challenged with *M.tb* (DPI 10 and 21) (Fig.6A and Sup. Fig.S5C). We focused on the expression of CD69 on CD4$^+$ and CD8$^+$ T cells, and the ability of T cells to produce IFNγ or IL-17A. In BCG and dBCG groups, the number of resident CD69 expressing CD4$^+$ and CD8$^+$ T cells in the lung before *M.tb* challenge was increased relative to vehicle but did not differ between BCG and dBCG vaccinated mice. Infection with *M.tb* increased the number of CD69$^+$CD4$^+$ and CD69$^+$CD8$^+$ T cells in the lung of

vehicle control mice, but the number of CD69+CD4+ and CD69+CD8+ T cells in the lung was enhanced further with dBCG at 21 DPI (Fig.6B). To further assess T cell activation in the lung we evaluated two important effector mechanisms required for *M.tb* control, the production of IFNγ and IL-17A by T cells [7,29–32]. Although the number of CD4+IFNγ+ and CD8+IFNγ+ T cells in the lung was elevated 50 DPV in BCG and dBCG vaccinated mice, we did not observe statistically significant increases in the number of CD4+IFNγ+ and CD8+IFNγ+ T cells in the lung between BCG- or dBCG-vaccinated mice at any time point post *M.tb* infection (Fig.6C). We did, however, observe significant increases in the number of CD4+IL-17A+ and CD8+IL-17A+ T cells in the lung (Fig.6D), with significant increases in the number of CD8+IL-17A+ T cells at 10 DPI and significant increases in CD4+IL-17A+ and CD8+IL-17A+ T cells at 21 DPI in the lung of dBCG-vaccinated mice.

Enhanced control of *M.tb* by dBCG is linked to IL-17A-associated responses during vaccination period

Having observed significant increases in the activation (CD69) and IL-17A, but not IFNγ, positive T cells in the lung of dBCG vaccinated mice infected with *M.tb*, we sought to evaluate whether these responses were antigen specific. Mice were vaccinated with BCG or dBCG, sacrificed at 50 DPV, and purified lung cells were cultured with a mixture of *M.tb*-derived antigens. Analysis of cell populations positive for CD69, IFNγ, or IL-17A after stimulation revealed a decreasing trend for the total percentage of IFNγ positive cells in the dBCG group and an increasing trend for the number of IL-17A positive ones, in both the CD4+ and CD8+ populations (Fig.7A, Sup. Fig.S8). This led us to hypothesize that the induction of IL-17A-associated responses is important for dBCG-mediated immunity. To directly assess whether IL-17A contributes to the control of *M.tb* following dBCG vaccination, mice were vaccinated with BCG or dBCG and injected with anti-IL-17A throughout the duration of the vaccination period beginning one day prior to vaccination, challenged with *M.tb*, and sacrificed at 21 DPI to assess bacterial burden (Fig.7B). As expected, naïve mice had the highest bacterial burden, and both vaccinations were able significantly reduce bacterial burden in the lung. However, as previously observed, dBCG was superior to BCG at reducing *M.tb* bacterial burden. Neutralization of IL-17A had no significant effect on the bacterial burden in the BCG group, but its neutralization in the dBCG group abolished the increased protection associated with dBCG vaccination (Fig.7C). Overall, our results suggest the non-polar lipid components of the mycobacterial cell wall negatively impact BCG's vaccine efficacy when delivered directly to the lungs, and directly implicates IL-17A as an important immune response modulator.

DISCUSSION

BCG remains the only vaccine available to prevent TB, yet it fails to confer long-term immunity against PTB. Despite its success against meningeal- and miliary-TB, BCG's efficacy against PTB must be improved if we wish to eradicate this disease. One underlying factor that may contribute to this phenomenon is the route of immunization with BCG, which does not reflect the route of natural infection with *M.tb*. *M.tb* has evolved to be a pulmonary pathogen by taking advantage of the immunoprivileged status of the lung, where inflammatory responses are tightly regulated to prevent excessive damaging inflammation

[33]. Vaccination with conventional BCG, on the other hand, is administered into the dermal layer of the skin [2]. Multiple studies have suggested that BCG is more efficacious against *M.tb* when delivered directly into the lung [5–7]. Unfortunately, the presence of immunomodulatory and inflammatory lipids on the mycobacterial cell wall has restrained the use of BCG as a pulmonary vaccine in humans. Previous studies by Silva et al.[11] and Indrigo et al.[34] demonstrated the importance of petroleum ether extracted mycobacterial lipids, especially TDM, in the host-pathogen relationship that takes place in infections caused by mycobacteria *in vitro* and *in vivo*. As a result, we postulated that selective removal of inflammatory lipids from the cell wall of BCG [11] would enable direct pulmonary vaccination with BCG.

Selective delipidation of BCG with PE effectively served as a more potent vaccine against *M.tb* when administered directly into the lungs. However, we acknowledge that dBCG still leads to increasing *M.tb* burden over time, but it does remain superior in its protection relative to conventional BCG, including reduced immunopathology. We thus suggest that by lowering initial lung inflammatory responses, we have identified an important improvement over conventional BCG. In this regard, pulmonary immunopathology is the primary reason why BCG has not been repurposed as a pulmonary vaccine [8,9] and immunopathology of *M.tb* infected animal models is a major correlate of morbidity and mortality [2].

Our data suggest that the improved protection and reduced pulmonary inflammation (to dBCG and *M.tb*) associated with dBCG vaccination is due to the removal of virulent lipids including TDM, MycB, PGL, TAGs, and PDIMs from the BCG cell wall, which can inhibit the development of effective immune responses and/or exacerbate inflammatory responses. In this context, TDM has been associated with the ability to inhibit fusion between phospholipid vesicles such as those required for the fusion of phagosomes with lysosomes [35]. Phagosome-lysosome fusion is required for the killing of intracellular *M.tb* and for the subsequent presentation of foreign peptides along with MHC class II to T cells [36]. TDM can also inhibit cellular energy metabolism [37], inhibit crosstalk between innate and adaptive immune cells [38], and induce apoptosis of lymphocytes [39]. Some *M.tb* clinical isolates can synthesize the trisaccharide form of PGL, which can inhibit Toll-like receptor 2 (TLR2)-induced NF-κB activation, and thus the production of IL-1β, TNF, and IL-6 [17]. Like PGL, the accumulation of TAGs on the mycobacterial cell surface can increase virulence [40]. PDIMs also appear to play a role in the virulence of mycobacteria as suggested by *M.tb* strains that lack PDIM being less virulent in mouse models [20,41], a phenotype attributed to reduced binding of *M.tb* to the plasma membrane of macrophages and increased phagosomal acidification [13]. Other studies have linked the absence of PDIMs on *M.tb* to reduced survival of *M.tb* within macrophages, suggesting PDIMs protect *M.tb* from early innate host responses [19]. Thus, delipidation of BCG has a significant impact on multiple virulence factors that influence both innate and adaptive immune elements.

We also anticipate that dBCG may begin rebuilding its cell wall soon after it enters an environment that is permissive to growth. However, mice vaccinated with dBCG had minimal pathology at 150 DPV in the lung, indicating that in the case that dBCG can resynthesize the removed lipids, this potential reconstitution does not induce the inflammatory response associated with conventional BCG. Moreover once dBCG is

inoculated, innate host cells may rapidly begin to kill the bacteria. This rapid killing, combined with a slow antigen presentation process, could explain why dBCG is more efficient at controlling *M.tb* growth. In this context, interestingly, at day 7, dBCG vaccination drove a transient decrease in nearly all innate cells studied. We attribute this decrease to the absence of inflammatory lipids on the dBCG cell wall, where dBCG could induce a transient cell turnover to exit the lung, or for the case of monocytes, it could accelerate their differentiation into lung macrophages (alveolar and/or interstitial) and/or dendritic cells. Conversely, the absence of immunomodulatory/inflammatory lipids in dBCG could also allow for the development of a stronger adaptive immune response by bypassing the masking effect that the presence of these lipids on conventional BCG may have.

Pulmonary vaccination with dBCG may also accelerate the development of immunological memory and T cell activation in the lung following *M.tb* infection. Although we observed a significant increase in the number of CD4 and CD8 T cells positive for CD69 in both BCG- and dBCG-vaccinated groups at 50 DPV and 10 DPI, dBCG-vaccinated mice had higher numbers of $CD4^+CD69^+$ and $CD8^+CD69^+$ T cells in the lung 21 DPI, suggesting that vaccination with dBCG may accelerate T cell activation upon *M.tb* infection. We also assessed the number of T cells capable of producing IFNγ and IL-17A in the lung, important cytokines for *M.tb* containment [42,43]. Unexpectedly, we did not observe any significant differences between BCG- and dBCG-vaccinated mice in the number of T cells capable of producing IFNγ prior to, or following, infection with *M.tb* in the lung. Furthermore, the overall proportion of IFNγ$^+$ T cells after stimulation with *M.tb* antigens was decreased in dBCG-vaccinated mice at the time of infection. Since IFNγ did not mediate the additional protection against *M.tb* associated with dBCG vaccination, we assessed whether IL-17A was implicated [30,42]. We observed significant increases in the number of $CD8^+IL-17A^+$ T cells in the lung of dBCG-vaccinated mice at 10 DPI, and significant increases in the number of $CD4^+IL-17A^+$ and $CD8^+IL-17A^+$ cells in the lung at 21 DPI. Furthermore, the proportion of T cells positive for IL-17A after *M.tb* antigen stimulation was higher in dBCG-vaccinated mice. Depletion of IL-17A from dBCG-vaccinated mice during the vaccination period confirmed its requirement for controlling *M.tb* bacterial burden in the lung. Thus, our data support that IFNγ may have a limited ability to protect against *M.tb* in the lung and that IL-17A responses may be necessary for effective vaccination-induced mycobacterial immunity in the lung.

The key to this novel approach could be the rapid innate immune response that occurs after inoculation, which helps to develop strong adaptive immune responses. Although the pathology observed post-*M.tb* infection is likely due to *M.tb*, we cannot rule out that residual BCG is also responsible. We also stress that the significance of these findings lies in the route of immunization. It may be difficult to justify the use of conventional BCG as a pulmonary vaccine due to large amounts of inflammation generated in the lungs. However, dBCG could offer a solution; a less cytotoxic vaccine that could be inoculated directly into the lungs and that is associated with greater immunopathological protection and subsequent delayed *M.tb* expansion. Additionally, targeting IFNγ responses may not necessarily increase immunity to mycobacteria in the lung. Instead, IL-17A responses may contribute significantly to mycobacterial immunity in the lung mucosa in the context of BCG vaccination.

Our data suggest that BCG cell wall lipids directly inhibit the generation of protective immune responses to *M.tb*. Whereas current vaccines typically fall under the categories of attenuated, inactivated, or subunit/conjugate, we have classified dBCG under a new category we named "selective attenuation". While the bacteria remain alive, and therefore capable of replenishing the extracted lipids on their cell walls, the removal of cell wall lipids significantly reduces its ability to survive within host cells. This allowed us to vaccinate via a more immunogenic route. Additionally, as high incidence of TB occurs in developing countries, particularly within rural communities that may lack access to routine health care, TB vaccine design should aim to develop single dose formulations. Vaccines that require administration of multiple components pose significant logistical challenges. For these reasons, our design was centered on developing a single-dose vaccine that can be safely delivered to the lung. We overcame both challenges via a simple lipid extraction using the readily available solvent petroleum ether. The procedure was fast, reproducible, inexpensive, and can be easily implemented into current vaccine production.

Further studies are required to determine the potential translation of our findings from mouse to humans. Logistically, dBCG may need to surpass the protective effects of conventional BCG in pre-clinical models. A ratio improvement of uninfected:latent infection:active TB disease in dBCG vaccinated NHPs could fast-track dBCG for vaccine production due to the urgency of addressing the current TB epidemic [44]. As dBCG seems to cause less burden and delays immunopathology, this vaccine may allow for routes of vaccination previously considered too toxic (*i.e.* the lung), as well as potentially addressing the current safety concerns of using conventional BCG for immunocompromised individuals. Altogether our research highlights the complexities of the initial interaction between mycobacteria and the host and exemplifies that a thorough understanding of the mycobacterial cell wall can lead to a better understanding of the requirements for effective mycobacterial immunity.

METHODS

Ethics statement.

All experimental procedures with animals were approved by the The Ohio State University IACUC (2012A00000132) and Texas Biomedical Research Institute AICUC (1611-MU). All mouse experiments were repeated at least twice (n=2) with 4–5 mice per group. For human subjects, this study was carried out in strict accordance with US Code of Federal and Local Regulations, Human Subjects IRB protocols: 2007H0262 and 2008H0119. Only healthy adult human subjects were recruited (50:50 F:M, 21–44 years old) with written informed consent.

Mice.

Specific-pathogen-free C57BL/6 female mice (Jackson-Laboratories, Bar Harbor, ME) aged 6–8 weeks were hosted as described [28,45]. Mice were divided into three groups: Mock-vaccinated (vehicle), PBS-treated-BCG-vaccinated (BCG), or PE-treated-BCG-vaccinated (dBCG). Each group contained 4–5 mice and experiments were repeated once for a total of 8–10 mice per group studied.

Growth conditions of mycobacteria and delipidation of M. bovis BCG strain Pasteur.

GFP-*M.tb* Erdman (provided by Dr. Horwitz, UCLA, CA) [46] and *M. bovis* BCG Pasteur strains [BCG, ATCC, #35734] were grown as previously described [47]. To delipidate BCG, freshly plated BCG was harvested between 9–14 days of growth into siliconated tubes (Fisher Scientific, Hampton, NH), suspended in 1 ml of PE or PBS and vortexed for two minutes, rested for five minutes, and then pelleted at 6000 g for five minutes. The procedure was performed as previously described [23,24] and repeated three times. The supernatants from the PE treated bacteria were collected, dried under N_2, and kept at −20°C until further analysis. Treated bacteria used for *in vitro* or *in vivo* studies were dried briefly in the biosafety cabinet to evaporate the excess solvent, washed with PBS, and suspended in PBS prior to use. The viability of BCG and dBCG was determined counting colonies three to four weeks later [47]. Generation of a viable single cell suspension of BCG after delipidation was confirmed by staining with a live/dead solution containing propidium iodide (535 nm) and SYTO®9 (485 nm) for ten minutes (ThermoFisher Scientific Cat. L7012). Bacteria were visualized under an Olympus FluoView FV10i confocal microscope at a final magnification of 600X with a 3X zoom.

Analysis of the extracted lipids.

To assess the remaining lipids on the cell wall of BCG post PE extraction, PE-treated bacteria were further extracted with C:M (2:1, v/v) at 37°C for 12 h. PE and C:M extracted lipids (spotted 100 μg per lane) were analyzed by TLC using aluminum-backed TLC plates with the following solvent systems: For TDM, MycB, and PGL (C:M 95:5, v/v); for PDIMs and TAGs (PE:acetone, 96:4, v/v); and PIMs (C:acetic acid:M:water, 40:25:3:6, v/v/v/v). TLC bands were visualized by first spraying the plates with 10% H_2SO_4 in H_2O followed by charring at 100°C. Developed TLCs were imaged using an Epson Perfection V600 photo scanner. Quantification was performed using the NIH software ImageJ. Total BCG extracts were obtained by sequential extractions using C:M (2:1, v/v); C:M (1:2, v/v) and C:M:water (10:10:3, v/v/v) as we previously reported [48].

Vaccination and M.tb aerosol infection.

C57BL/6 mice were anesthetized with an aerosolized solution containing 2–5% isoflurane. A single cell suspension of BCG or dBCG containing approximately 5×10^5 viable bacilli in 50 μl was intranasally administrated evenly between the two nares allowing for inhalation into the lungs one mouse at a time. Following administration, mice were held in an upright position for 15 seconds to ensure the entire inoculum was inhaled. For *M.tb* studies, mice were infected via aerosol with a low dose of *M.tb* using the Glas-Col (Terre Haute, IN) inhalation exposure system as we described [28,45].

Histopathology.

Lung tissue sections were prepared, processed and analyzed as described by a board-certified veterinarian in a blinded manner [45].

In vitro infection of human macrophages.

In vitro infections were performed as described previously. For specific details, see supplementary materials.

Lung cell isolation.

Lung cells were isolated as previously described [49]. Cell suspensions were counted using Trypan blue to exclude dead cells and resuspended at a working concentration in c-DMEM or fixed for flow cytometry.

Immunophenotyping by flow cytometry.

Lung cells were prepared for flow cytometry as described previously [45]. For specific details, see supplementary materials.

Neutralization of IL-17A.

IL-17A (500 μg; Clone: 17F3; BioXCell, West Lebanon, NH) depletion antibody or whole mouse IgG1, k (500 μg; Clone: MOPC-21; BioXCell) isotype control were administered in 100 μl into the intraperitoneal cavity twelve times over a period of 50 days beginning one day prior to vaccination and ending three days prior to *M.tb* challenge.

Statistical analysis.

Statistical significance was determined using Prism 7 software (GraphPad). The unpaired, two-tailed Student's *t*-test was used for two group comparisons. Multiple comparisons were analyzed using one-way ANOVA with the Holm-Sidak's multiple comparison test to compare all groups against control (naïve) (*), groups within the same time points (#), and groups across different time points (§). Statistical significance was reported as *,§,# $p < 0.05$; **,§§,## $p < 0.01$; ***,§§§,### $p < 0.001$; ****$p < 0.0001$.

Supplementary Material

Refer to Web version on PubMed Central for supplementary material.

ACKNOWLEDGEMENTS

REFERENCES

1. WHO. Global Tuberculosis Report 2018. 1–277 (WHO Organization, Geneva, 2018). http://apps.who.int/iris/bitstream/handle/10665/274453/9789241565646-eng.pdf?ua=1

2. Moliva JI, Turner J & Torrelles JB Prospects in Mycobacterium bovis Bacille Calmette et Guerin (BCG) vaccine diversity and delivery: Why does BCG fail to protect against tuberculosis? Vaccine 33, 5035–5041, doi:S0264–410X(15)01159–7 [pii];10.1016/j.vaccine.2015.08.033 [doi] (2015). [PubMed: 26319069]

3. Moliva JI, Turner J & Torrelles JB Immune responses to BCG vaccination: Why do they fail to protect against Mycobacterium tuberculosis? Front Immunol 8, 407 (2017). [PubMed: 28424703]

4. Lambert PH & Laurent PE Intradermal vaccine delivery: will new delivery systems transform vaccine administration? Vaccine 26, 3197–3208, doi:S0264–410X(08)00391–5 [pii];10.1016/j.vaccine.2008.03.095 [doi] (2008). [PubMed: 18486285]

5. Derrick SC, Kolibab K, Yang A & Morris SL Intranasal administration of *Mycobacterium bovis* BCG induces superior protection against aerosol infection with *Mycobacterium tuberculosis* in mice. Clin. Vaccine Immunol 21, 1443–1451, doi:CVI.00394–14 [pii];10.1128/CVI.00394-14 [doi] (2014). [PubMed: 25143340]

6. Perdomo C et al. Mucosal BCG vaccination induces protective lung-resident memory T cell populations against tuberculosis. MBio 7, doi:mBio.01686–16 [pii];10.1128/mBio.01686-16 [doi] (2016).

7. Aguilo N et al. Pulmonary but not subcutaneous delivery of BCG vaccine confers protection to tuberculosis-susceptible mice by an Interleukin 17-dependent mechanism. J Infect. Dis 213, 831–839, doi:jiv503 [pii];10.1093/infdis/jiv503 [doi] (2016). [PubMed: 26494773]

8. Tree JA et al. Intranasal bacille Calmette-Guerin (BCG) vaccine dosage needs balancing between protection and lung pathology. Clin. Exp. Immunol 138, 405–409, doi:CEI2648 [pii];10.1111/j.1365-2249.2004.02648.x [doi] (2004). [PubMed: 15544615]

9. Nuermberger EL, Yoshimatsu T, Tyagi S, Bishai WR & Grosset JH Paucibacillary tuberculosis in mice after prior aerosol immunization with Mycobacterium bovis BCG. Infect. Immun 72, 1065–1071 (2004). [PubMed: 14742554]

10. Geisel RE, Sakamoto K, Russell DG & Rhoades ER In vivo activity of released cell wall lipids of Mycobacterium bovis bacillus Calmette-Guerin is due principally to trehalose mycolates. J Immunol 174, 5007–5015, doi:174/8/5007 [pii] (2005). [PubMed: 15814731]

11. Silva CL, Ekizlerian SM & Fazioli RA Role of cord factor in the modulation of infection caused by mycobacteria. Am J Pathol 118, 238–247 (1985). [PubMed: 3881973]

12. Chauhan P et al. Secretory phosphatases deficient mutant of *Mycobacterium tuberculosis* imparts protection at the primary site of infection in guinea pigs. PLoS. ONE 8, e77930, doi:10.1371/journal.pone.0077930 [doi];PONE-D-13–13242 [pii] (2013). [PubMed: 24205032]

13. Astarie-Dequeker C et al. Phthiocerol dimycocerosates of *M. tuberculosis* participate in macrophage invasion by inducing changes in the organization of plasma membrane lipids. PLoS. Pathog 5, e1000289, doi:10.1371/journal.ppat.1000289 [doi] (2009). [PubMed: 19197369]

14. Sinsimer D et al. The phenolic glycolipid of *Mycobacterium tuberculosis* differentially modulates the early host cytokine response but does not in itself confer hypervirulence. Infect. Immun 76, 3027–3036, doi:IAI.01663–07 [pii];10.1128/IAI.01663-07 [doi] (2008). [PubMed: 18443098]

15. Cambier CJ, O'Leary SM, O'Sullivan MP, Keane J & Ramakrishnan L Phenolic glycolipid facilitates mycobacterial escape from microbicidal tissue-resident macrophages. Immunity 47, 552–565 e554, doi:10.1016/j.immuni.2017.08.003 (2017). [PubMed: 28844797]

16. Reed MB et al. A glycolipid of hypervirulent tuberculosis strains that inhibits the innate immune response. Nature 431, 84–87 (2004). [PubMed: 15343336]

17. Arbues A, Lugo-Villarino G, Neyrolles O, Guilhot C & Astarie-Dequeker C Playing hide-and-seek with host macrophages through the use of mycobacterial cell envelope phthiocerol dimycocerosates and phenolic glycolipids. Front Cell Infect. Microbiol 4, 173, doi:10.3389/fcimb.2014.00173 [doi] (2014). [PubMed: 25538905]

18. Arbues A et al. Trisaccharides of phenolic glycolipids confer advantages to pathogenic mycobacteria through manipulation of host-cell pattern-recognition receptors. ACS Chem. Biol 11, 2865–2875, doi:10.1021/acschembio.6b00568 [doi] (2016). [PubMed: 27548027]

19. Day TA et al. *Mycobacterium tuberculosis* strains lacking surface lipid phthiocerol dimycocerosate are susceptible to killing by an early innate host response. Infect. Immun 82, 5214–5222, doi:IAI.01340–13 [pii];10.1128/IAI.01340-13 [doi] (2014). [PubMed: 25287926]

20. Cox JS, Chen B, McNeil M & Jacobs WR Jr. Complex lipid determines tissue-specific replication of *Mycobacterium tuberculosis* in mice. Nature 402, 79–83 (1999). [PubMed: 10573420]

21. Tran V, Ahn SK, Ng M, Li M & Liu J Loss of lipid virulence factors reduces the efficacy of the BCG vaccine. Sci. Rep 6, 29076, doi:srep29076 [pii];10.1038/srep29076 [doi] (2016). [PubMed: 27357109]

22. Indrigo J, Hunter RL Jr. & Actor JK Cord factor trehalose 6,6'-dimycolate (TDM) mediates trafficking events during mycobacterial infection of murine macrophages. Microbiology 149, 2049–2059 (2003). [PubMed: 12904545]

23. Bloch H Studies on the virulence of tubercle bacilli: Isolation and biological properties of a constituent of virulent organisms. J. Exp. Med 91, 197–219 (1950). [PubMed: 15404225]

24. Noll H, Bloch H, Asselineau J & Lederer E The chemical structure of the cord factor of *Mycobacterium tuberculosis*. Biochim Biophys Acta 20, 299–309 (1956). [PubMed: 13328853]

25. Smith KC, Orme IM & Starke JR in Vaccines Ch. 35, 789–811 (Saunders, 2012).

26. Vogelzang A et al. Central memory CD4+ T cells are responsible for the recombinant Bacillus Calmette-Guerin DeltaureC::hly vaccine's superior protection against tuberculosis. J. Infect. Dis, doi:jiu347 [pii];10.1093/infdis/jiu347 [doi] (2014).

27. Mueller SN, Gebhardt T, Carbone FR & Heath WR Memory T cell subsets, migration patterns, and tissue residence. Annu. Rev. Immunol 31, 137–161, doi:10.1146/annurev-immunol-032712-095954 [doi] (2013). [PubMed: 23215646]

28. Cyktor JC, Carruthers B, Beamer GL & Turner J Clonal Expansions of CD8(+) T Cells with IL-10 secreting capacity occur during chronic Mycobacterium tuberculosis infection. PLoS. ONE 8, e58612, doi:10.1371/journal.pone.0058612 [doi];PONE-D-12–40405 [pii] (2013). [PubMed: 23472214]

29. Flynn JL et al. An essential role for interferon gamma in resistance to *Mycobacterium tuberculosis* infection. J. Exp. Med 178, 2249–2254 (1993). [PubMed: 7504064]

30. Khader SA et al. IL-23 and IL-17 in the establishment of protective pulmonary CD4+ T cell responses after vaccination and during *Mycobacterium tuberculosis* challenge. Nat. Immunol 8, 369–377 (2007). [PubMed: 17351619]

31. Effros RB & Walford RL Diminished T-cell response to influenza virus in aged mice. Immunology 49, 387–392 (1983). [PubMed: 6602091]

32. Cooper AM et al. Disseminated tuberculosis in interferon gamma gene-disrupted mice. J. Exp. Med 178, 2243–2247 (1993). [PubMed: 8245795]

33. Cooper AM Cell-mediated immune responses in tuberculosis. Annu. Rev. Immunol 27, 393–422 (2009). [PubMed: 19302046]

34. Indrigo J, Hunter RL Jr. & Actor JK Influence of trehalose 6,6'-dimycolate (TDM) during mycobacterial infection of bone marrow macrophages. Microbiology 148, 1991–1998, doi:10.1099/00221287-148-7-1991 (2002). [PubMed: 12101287]

35. Spargo BJ, Crowe LM, Ioneda T, Beaman BL & Crowe JH Cord factor (a,a-trehalose 6,6'-dimycolate) inhibits fusion between phospholipid vesicles. Proc. Natl. Acad. Sci. USA 88, 737–740 (1991). [PubMed: 1992465]

36. Pieters J *Mycobacterium tuberculosis* and the macrophage: Maintaining a balance. Cell Host. Microbe 3, 399–407, doi:S1931–3128(08)00154–6 [pii];10.1016/j.chom.2008.05.006 [doi] (2008). [PubMed: 18541216]

37. Fox CJ, Hammerman PS & Thompson CB Fuel feeds function: Energy metabolism and the T-cell response. Nat. Rev. Immunol 5, 844–852, doi:nri1710 [pii];10.1038/nri1710 [doi] (2005). [PubMed: 16239903]

38. Kan-Sutton C, Jagannath C & Hunter RL Jr. Trehalose 6,6'-dimycolate on the surface of *Mycobacterium tuberculosis* modulates surface marker expression for antigen presentation and costimulation in murine macrophages. Microbes. Infect 11, 40–48, doi:S1286–4579(08)00284–0 [pii];10.1016/j.micinf.2008.10.006 [doi] (2009). [PubMed: 19007905]

39. Ozeki Y et al. In vivo induction of apoptosis in the thymus by administration of mycobacterial cord factor (trehalose 6,6'-dimycolate). Infect. Immun 65, 1793–1799 (1997). [PubMed: 9125563]

Author Manuscript

40. Reed MB, Gagneux S, Deriemer K, Small PM & Barry CE III. The W-Beijing lineage of *Mycobacterium tuberculosis* overproduces triglycerides and has the DosR dormancy regulon constitutively upregulated. J Bacteriol 189, 2583–2589 (2007). [PubMed: 17237171]

41. Cox D, Tseng CC, Bjekic G & Greenberg SA A requirement for phosphatidylinositol 3-kinase in pseudopod extension. J. Biol. Chem 274, 1240–1247 (2000).

42. Gopal R et al. Unexpected role for IL-17 in protective immunity against hypervirulent Mycobacterium tuberculosis HN878 infection. PLoS. Pathog 10, e1004099, doi:10.1371/journal.ppat.1004099 [doi];PPATHOGENS-D-13–03396 [pii] (2014). [PubMed: 24831696]

43. Pitt JM et al. Blockade of IL-10 signaling during bacillus Calmette-Guerin vaccination enhances and sustains Th1, Th17, and innate lymphoid IFN-gamma and IL-17 responses and increases protection to *Mycobacterium tuberculosis* infection. J. Immunol 189, 4079–4087, doi:jimmunol. 1201061 [pii];10.4049/jimmunol.1201061 [doi] (2012). [PubMed: 22972927]

44. Fauci AS Addressing the Tuberculosis Epidemic: 21st Century Research for an Ancient Disease. JAMA 320, 1315–1316, doi:10.1001/jama.2018.12852 (2018). [PubMed: 30267054]

45. Moliva JI et al. Exposure to human alveolar lining fluid enhances Mycobacterium bovis BCG vaccine efficacy against Mycobacterium tuberculosis infection in a CD8+ T-cell-dependent manner. Mucosal Immunol, doi:10.1038/mi.2017.80 (2017).

46. Tullius MV, Harth G & Horwitz MA High extracellular levels of *Mycobacterium tuberculosis* glutamine synthetase and superoxide dismutase in actively growing cultures are due to high expression and extracellular stability rather than to a protein-specific export mechanism. Infect. Immun 69, 6348–6363, doi:10.1128/IAI.69.10.6348-6363.2001 [doi] (2001). [PubMed: 11553579]

47. Arcos J et al. Human lung hydrolases delineate *Mycobacterium tuberculosis*-macrophage interactions and the capacity to control infection. J. Immunol 187, 372–381 (2011). [PubMed: 21602490]

48. Torrelles JB et al. Identification of *Mycobacterium tuberculosis* clinical isolates with altered phagocytosis by human macrophages due to a truncated lipoarabinomannan. J. Biol. Chem 283, 31417–31428 (2008). [PubMed: 18784076]

49. Canan CH et al. Characterization of lung inflammation and its impact on macrophage function in aging. J. Leukoc. Biol 96, 473–480, doi:jlb.4A0214–093RR [pii];10.1189/jlb.4A0214-093RR [doi] (2014). [PubMed: 24935957]
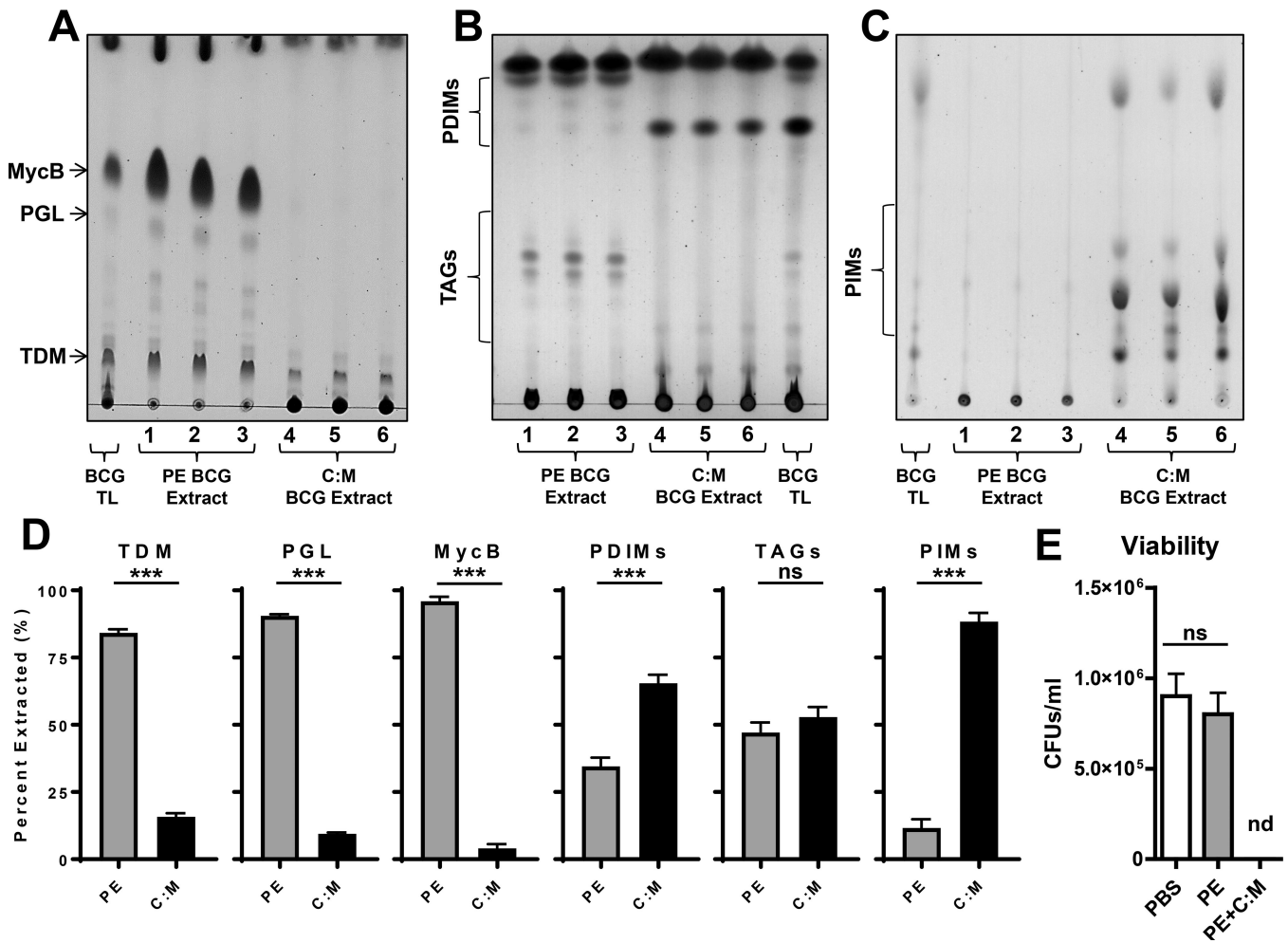
Figure 1. Petroleum ether extracts TDM, PGL, MycB, PDIMs, and TAGs without affecting the viability of BCG.

To assess nature and percentage of the lipids remaining on the BCG cell wall following extraction with PE (PE BCG extract), PE treated BCG was subjected to C:M (2:1, v/v) extraction for 12 h at 37°C (C:M BCG extract) (*n*=3; TLC, C:M, 95:5 v/v). Representative TLC images of PE BCG extracts in triplicate. BCG total lipid (BCG TL) extracts were included as a reference. (**A**) TDM, MycB, and PGL are highly extractable by PE. (**B**) Some PDIMs and TAGs are extracted from BCG by PE (*n*=3; TLC, petroleum ether/acetone, 96:4 v/v). (**C**) PIMs are not extractable by PE (*n*=3, TLC, chloroform/acetic acid/methanol/water, 40:25:3:6 v/v/v/v). (**D**) Densitometry analysis of all lipids plotted as percent extracted following treatment with the corresponding solvents, (PE BCG extracts, grey bars), (C:M BCG extracts, black bars), (*n*=3). (**E**) The viability of BCG treated with PBS, PE or C:M (2:1, v/v) assessed by plating serial dilutions (*n*=6). Representative experiment shown, each experiment performed at least three times, mean ± SEM; unpaired Student's *t*-test, ***$p<0.001$; ns: not significant, nd: no detected.
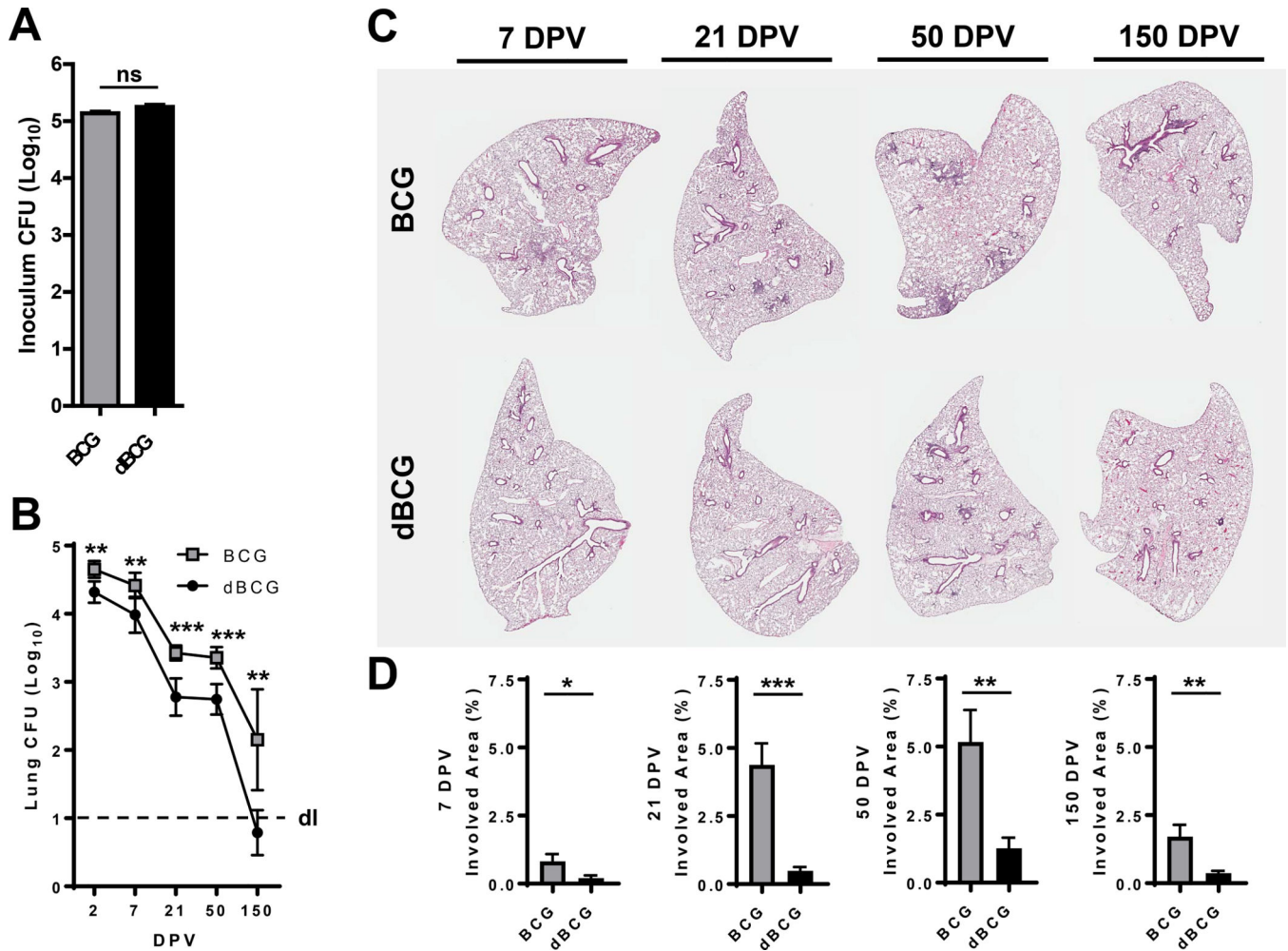
Figure 2. Delipidated BCG is quickly eliminated from the lung and is associated with reduced pathology of the lung.

C57BL/6J mice were intranasally inoculated with 5×10^5 viable BCG (grey bar or grey circle) or dBCG (black bar or black circle) bacilli. Mice were sacrificed at 2, 7, 21, 50, and 150 DPV to assess BCG bacterial burden in the lung. (**A**) Inoculum (*i.e.* the number of bacteria delivered into the lung) used to vaccinate mice showed no significant differences between the two groups. Representative experiment of *n*=2, mean ± SEM; unpaired Student's *t*-test; ns: not significant. (**B**) BCG CFUs in the lung assessed at 2, 7, 21, 50, and 150 DPV. Pooled results from *n*=2 with 4–5 mice/group per time-point, mean and error ± 95% CI; unpaired Student's *t*-test, **p<0.01, ***p<0.001. (**C**) Representative images of lung tissue at 7, 21, 50, and 150 DPV. (**D**) Areas of cell aggregation and infiltration (inflammation) in BCG (grey bars) or dBCG (black bars) vaccinated mice were quantified using Aperio Imagescope by calculating the area of inflammatory foci (*i.e.* involvement) divided by the total area of the lung. Representative images at a final magnification of 20X. Representative experiment from *n*=2 with 4–5 mice/group, mean ± SEM; unpaired Student's *t*-test, *p<0.05, **p<0.01, ***p<0.001.
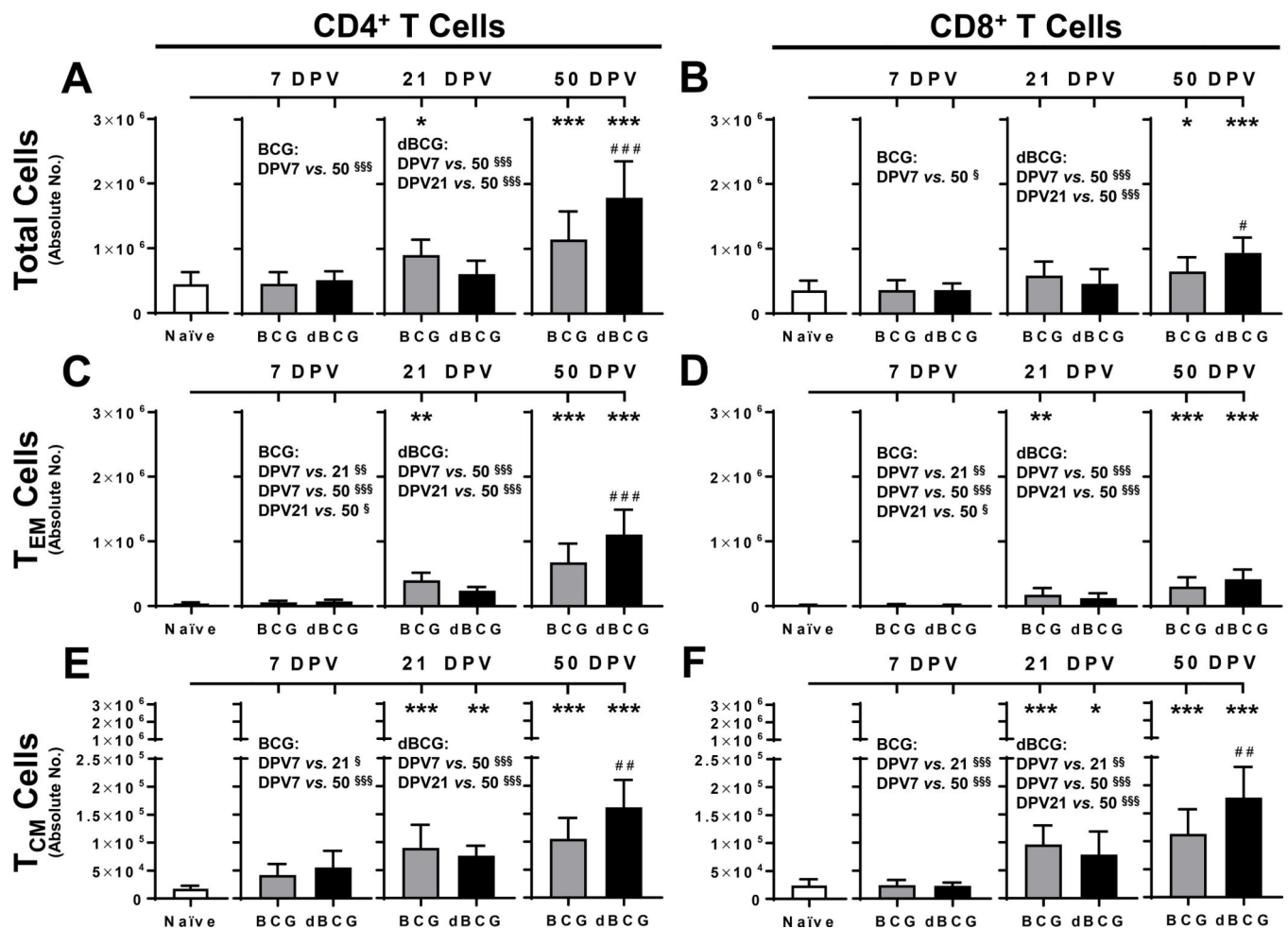
Figure 3. Pulmonary vaccination with delipidated BCG increases memory and effector T cell responses in the lung.

C57BL/6J mice were intranasally inoculated with 5×10^5 viable BCG (grey squares) or dBCG (black circles) bacilli. A group of naïve mice (white circles) was included as a control. Mice were sacrificed at 7, 21, and 50 DPV to characterize memory T cell responses in the lung. Total number of (**A**) CD4$^+$ and (**B**) CD8$^+$ T cells in the lung across time. The proportion of (**C**) CD4$^+$ or (**D**) CD8$^+$ effector T cells (CD62L$^-$CD44$^+$) increased across time and reached statistical significance in dBCG vaccinated mice at 50 DPV. The proportion of (**E**) CD4$^+$ or (**F**) CD8$^+$ memory T cells (CD62L$^+$CD44$^+$) also increased over time and peaked at 50 DPV in dBCG vaccinated mice. Pooled experiment from n=2 with 4–5 mice/group, mean ± SEM; One-way ANOVA with the Holm-Sidak's multiple comparison test. The bar on the top compares each group across time with the control group (naïve) (*p<0.05; **p<0.01; ***p<0.001). Comparisons among BCG or dBCG groups across time points is represented by the symbol § (§p<0.05; §§p<0.01; §§§p<0.001). Comparisons between groups at the same time point are represented by the symbol # (#p<0.05; ##p<0.01; ###p<0.001). Where not stated, it was not significant. For clarity, statistically significant comparisons across time points within the same group (BCG or dBCG) has been written within the figure (i.e. BCG: DPV7 vs. 21 §§p<0.01). DPV: day post vaccination.
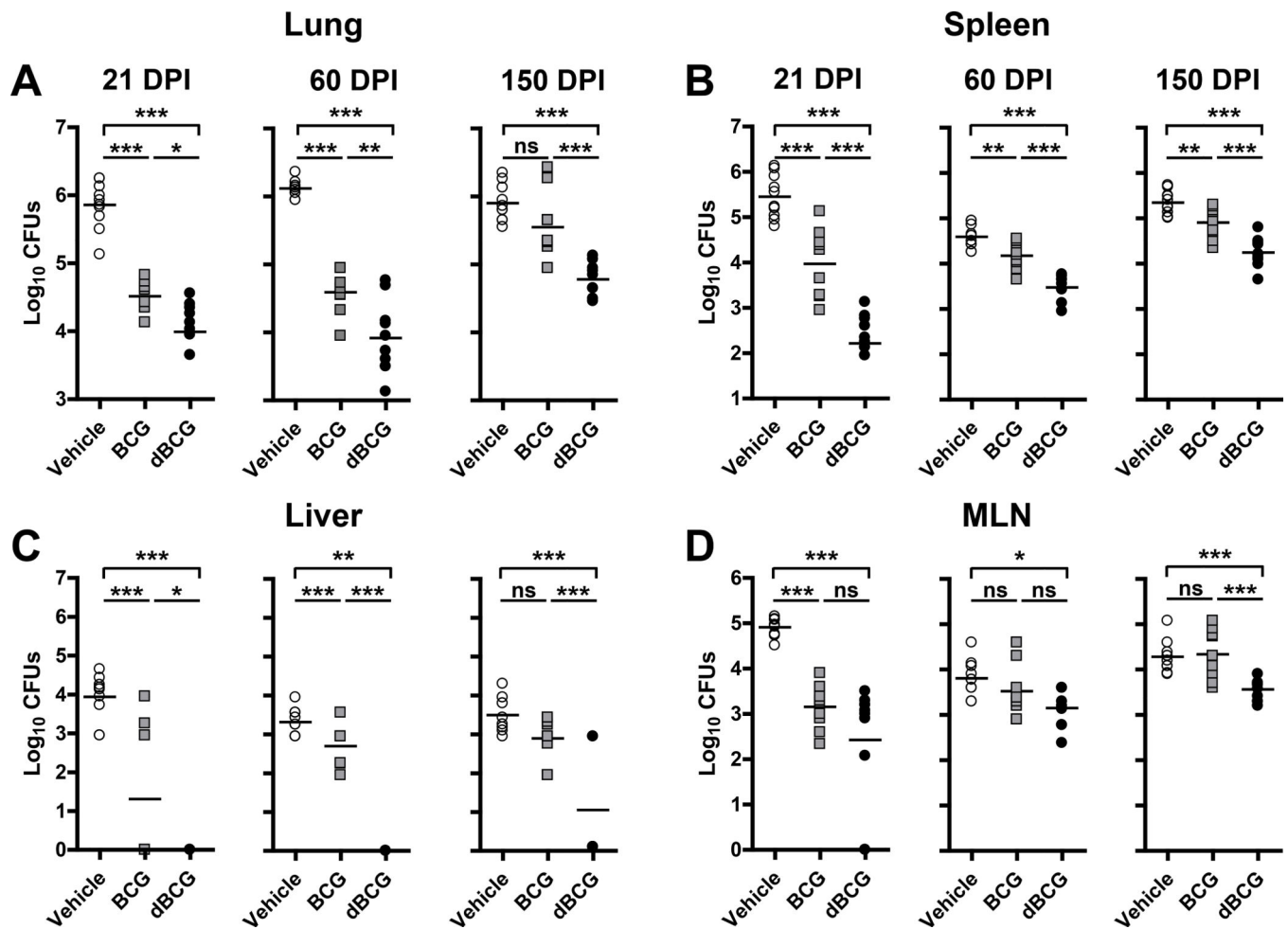
Figure 4. Pulmonary vaccination with dBCG reduces *M.tb* bacterial burden in the lung and peripheral organs of infected mice.

C57BL/6J mice were intranasally inoculated with PBS (vehicle; white circles) or 5×10^5 viable BCG (grey squares) or dBCG (black circles) bacilli. Fifty days later, mice were infected with a low dose aerosol of *M.tb*. At 21, 60, and 150 DPI mice were euthanized to assess bacterial burden in the (**A**) lung, (**B**) spleen, (**C**) liver, and (**D**) MLN. Colony counts reported are from experiments in which *M.tb* was grown in 7H11 agar supplemented with TCH which allows for the growth of *M.tb*, but not BCG. Pooled results from $n=2$ with 4–5 mice/group per time-point, mean ± SEM; One-way ANOVA with Tukey's post-hoc test, *$p<0.05$, **$p<0.01$, ***$p<0.001$; ns: not significant; MLN: mediastinal lymph node.
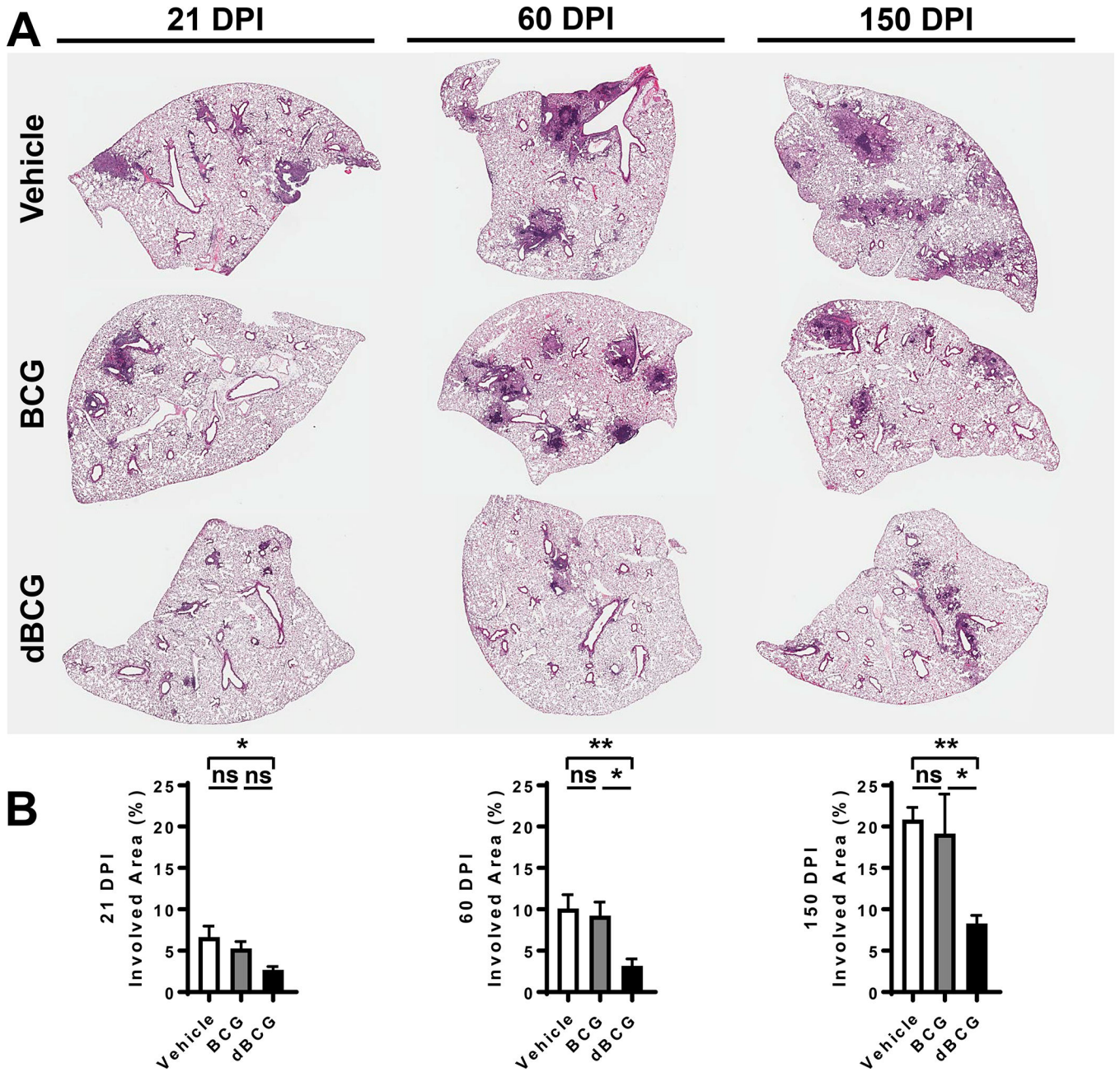
Figure 5. Pulmonary vaccination with dBCG is associated with decreased *M.tb* lung pathology across time.

C57BL/6J mice were intranasally inoculated with PBS (vehicle) or 5×10^5 viable BCG or dBCG bacilli. Fifty days later, mice were infected with a low dose aerosol of *M.tb*. (**A**) At 21, 60, and 150 DPI mice were sacrificed, and lungs fixed in 10% NBF, embedded in paraffin, sectioned, and stained with hematoxylin and eosin to visualize tissue morphology. (**B**) Areas of cell aggregation and infiltration (inflammation) in vehicle (white bars), BCG (grey bars) or dBCG (black bars) vaccinated mice were quantified using Aperio Imagescope by calculating the area of inflammatory foci (*i.e.* involvement) divided by the total area of the lung. Representative images at a final magnification of 20X. Pooled results from *n*=2

with 4–5 mice/group per time-point, mean ± SEM; One-way ANOVA with Tukey's post-hoc test, *p<0.05, **p<0.01; ns: not significant.
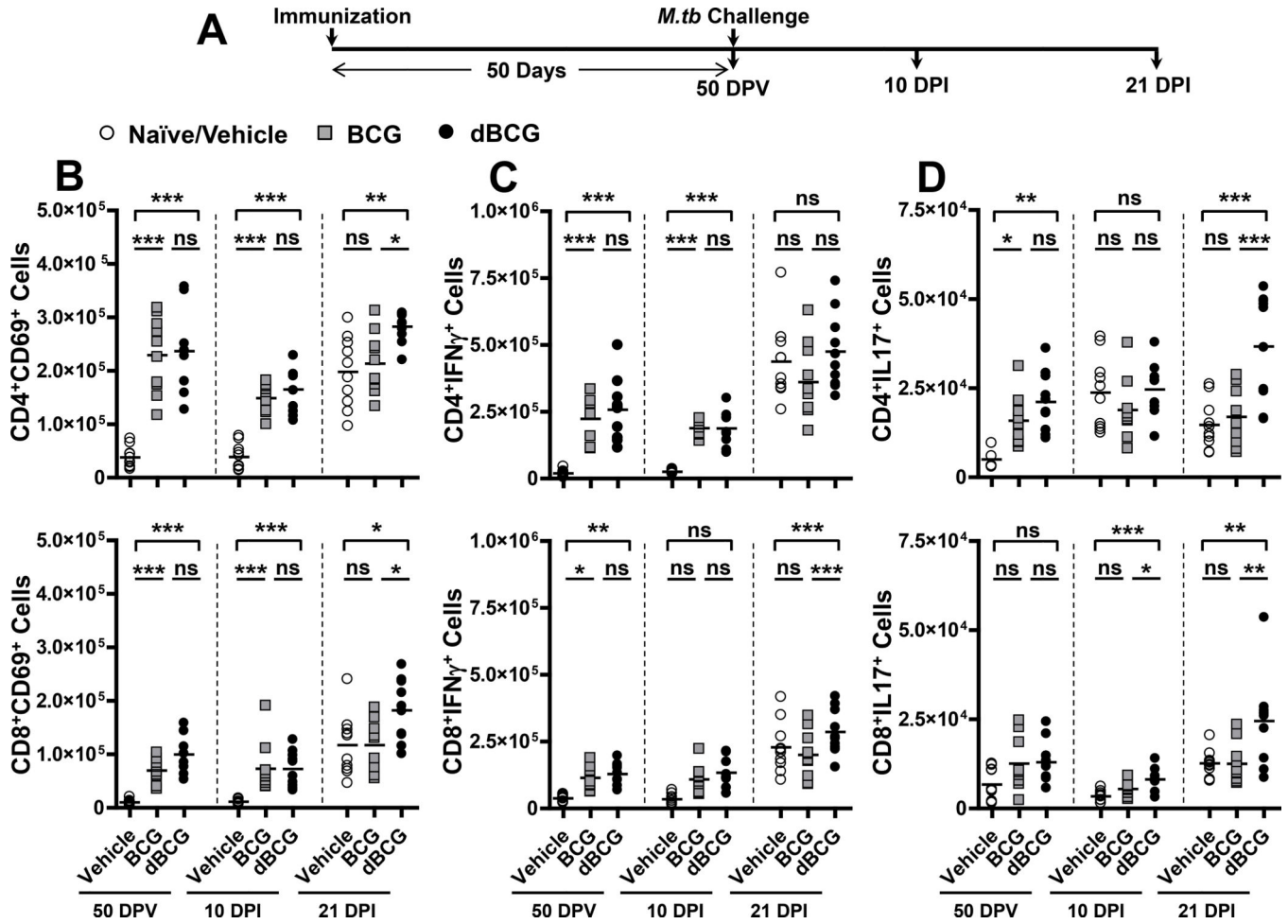
Figure 6. Pulmonary vaccination with dBCG boosts CD69 and IL-17A, but not IFNγ, responses in the lung of *M.tb* infected mice.
(**A**) Timeline showing experimental design. C57BL/6J mice were intranasally inoculated with vehicle (white circle) or 5×10^5 viable BCG (grey square) or dBCG (black diamond) bacilli. (**B**) T cell activation based on the expression of CD69 on CD4$^+$ and CD8$^+$ T cells at 50 DPV and at 10 and 21 DPI. CD69 was significantly increased in dBCG-vaccinated mice at 21 DPI. (**C**) Total number of CD4$^+$ and CD8$^+$ T cells staining positive for IFNγ after stimulation with CD3/CD28 in the presence of monensin. (**D**) Total number of CD4$^+$ and CD8$^+$ T cells staining positive for or IL-17A after stimulation with CD3/CD28 in the presence of monensin. Mice vaccinated with dBCG had significantly higher proportions of CD8$^+$IL-17A$^+$ cells (10 DPI) and CD4$^+$IL-17A$^+$ and CD8$^+$IL-17A$^+$ (21 DPI) in the lung, while IFNγ^+ cells were not significantly elevated in either vaccination group. Pooled experiment from *n*=2 with 4–5 mice/group, mean ± SEM; One-way ANOVA with Tukey's post-hoc test, *p<0.05, **p<0.01, ***p<0.001.
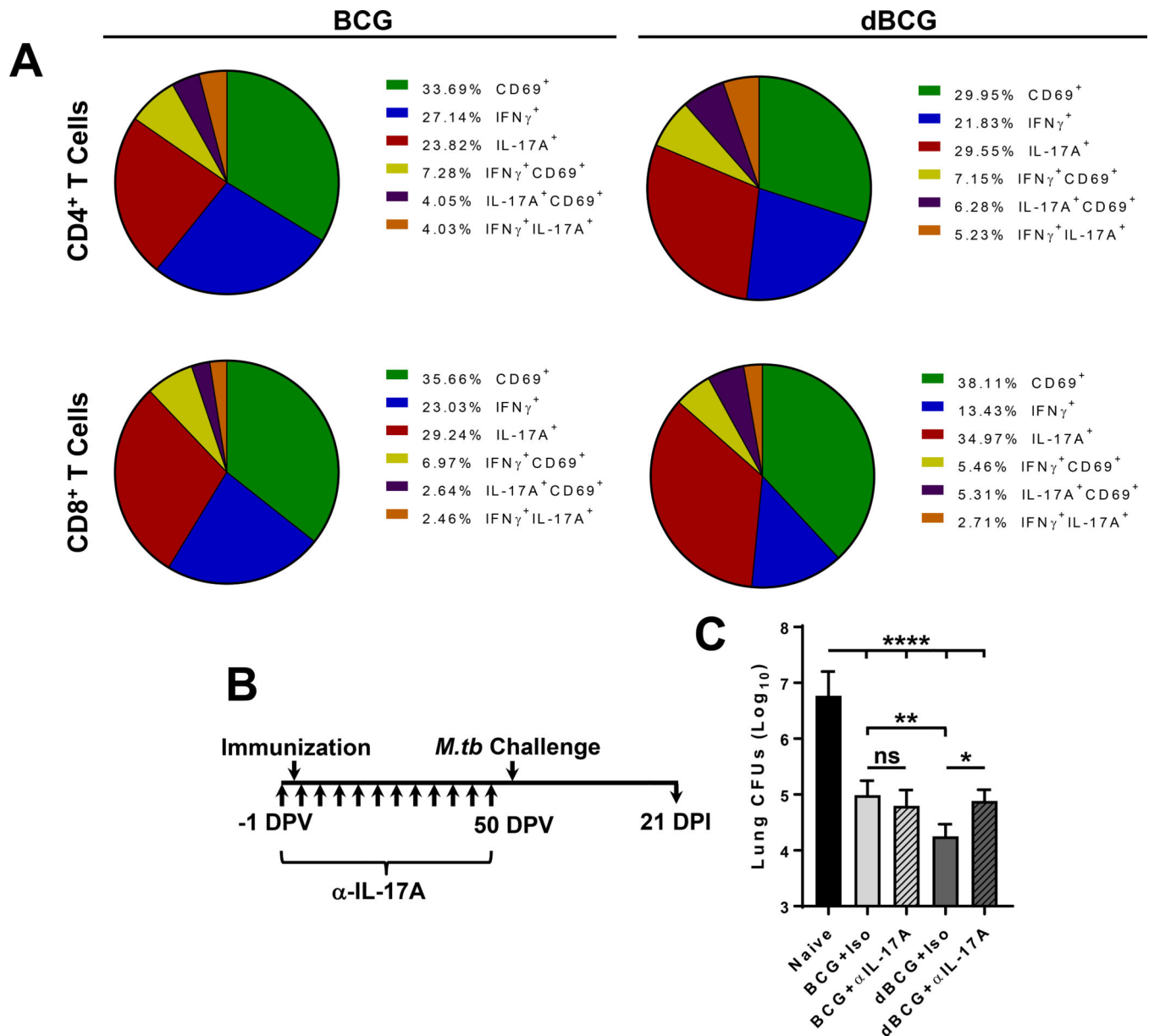
Figure 7. IL-17A is an important mediator of the increased efficacy of dBCG against *M.tb*.
(**A**) Purified lung cells of BCG or dBCG immunized mice sacrificed at 50 DPV were cultured with *M.tb* H$_{37}$R$_v$ CFP (10 μg) for 18h. The expression of CD69, IFNγ, and IL-17A was measured by flow cytometry. Each slice represents cells (CD4 or CD8) that express the corresponding molecule(s) as a percentage of the total number of cells analyzed. Overall, IFNγ responses were less prominent in dBCG-immunized mice, while IL-17A responses were elevated. (**B**) Timeline depicting experimental design for IL-17A neutralization. C57BL/6J mice were intranasally inoculated with vehicle (naïve) or 5×10^5 viable BCG or dBCG bacilli. IL-17A was depleted throughout the 50 day vaccination period beginning one day before vaccinations and was stopped three days prior to *M.tb* infection. (**C**) *M.tb* bacterial burden in the lung of naïve, BCG, or dBCG vaccinated mice injected with isotype or anti-IL-17A antibodies. Absence of vaccination (naïve, black bar) results in the highest

bacterial burden. Vaccination with BCG (light gray) reduced bacterial burden, while vaccination with dBCG (dark gray) reduced it even further. Depletion of IL-17A had no observable effect in the BCG group but ablated the additional protection associated with dBCG (dashed bars). Colony counts reported are from experiments in which *M.tb* was grown on 7H11 agar supplemented with TCH which allows for the growth of *M.tb*, but not BCG. Pooled results from n=2 with 4–5 mice/group per time-point, mean ± SEM; One-way ANOVA with Tukey's post-hoc test, *p<0.05, **p<0.01, ****p<0.0001, ns: not significant. Note: Open line with multiple dashes compares the naïve group with all the other groups showing in all cases the same significance (****p<0.0001).